Magnetic ordering in blocking layer and highly anisotropic electronic structure of high-T_c iron-based superconductor $Sr_2VFeAsO_3$: LDA+U study

Hiroki Nakamura[1,2,3,*] and Masahiko Machida[1,2,3,†]

[1]*CCSE, Japan Atomic Energy Agency, 6-9-3 Higashi-Ueno, Taito-ku, Tokyo 110-0015, Japan*

[2]*CREST, JST, 4-1-8 Honcho, Kawaguchi, Saitama 332-0012, Japan*

[3]*Transformative Research-Project on Iron Pnictides (TRIP), JST, Chiyoda, Tokyo 102-0075, Japan*

(Received 5 May 2010; revised manuscript received 30 July 2010; published 2 September 2010)

We calculate electronic structures of a high-T_c iron-based superconductor $Sr_2VFeAsO_3$ by local-density approximation (LDA) plus U method. We assume a checkerboard antiferromagnetic order on its blocking layers including vanadium and strong correlation in d orbits of vanadium through the Hubbard U. While the standard LDA brings about metallic blocking layers and complicated Fermi surface as in the previous literatures, our calculation changes the blocking layer into insulating one and the Fermi surface becomes quite similar to those of other iron-based superconductors. Moreover, the appearance of the insulating blocking layers suggests high anisotropy on quasiparticle transports as experimental results and predicts new types of intrinsic Josephson effects.

DOI: 10.1103/PhysRevB.82.094503 PACS number(s): 74.25.Jb, 71.15.Mb, 74.70.−b

Since the discovery of high-T_c superconductivity in $LaFeAsO_{1-x}F_x$,[1] its various family members have been piled up on the materials table of iron-based superconductors. The materials variety is characterized by their crystal structures and often classified by the numbering scheme, such as "1111" (e.g., $LaFeAsO_{1-x}F_x$), "122" [e.g., $Ba_{1-x}K_xFe_2As_2$ (Ref. 2)], "111" [e.g., LiFeAs (Ref. 3)], and "11" [e.g., FeSe (Ref. 4)]. They have quasi-two-dimensional FeAs layers commonly while the variety mainly comes from the nonsuperconducting blocking layers between the FeAs layers. The density-functional theory with local-density approximation (LDA) has predicted a common electronic structure, i.e., multiple cylindrical Fermi surfaces consisting of hole pockets around the Brillouin-zone center and electron ones around the zone corners. Some experiments, e.g., angle-resolved photoemission spectroscopy (ARPES) have actually confirmed such an electronic structure.[5] In this case, a strong candidate of the glue of their superconducting pairs has been regarded to be a spin fluctuation due to the nesting between those Fermi pockets,[6] though it still remains unsettled.

Recently, a new family who has a considerably thick perovskite-type blocking layer has been discovered[7] and a controversial debate about the pairing mechanism has arisen.[8–11] These materials include noniron transition-metal elements in their thick blocking layers, and the electronic structures can be relatively more complex than the other types, if 3d orbitals on the transition metals hybridize with Fe d orbitals. Such hybridization can clearly break the typical stage composed of disconnected small hole and electron pockets. $Sr_2VFeAsO_3$ is one of such perovskite-type iron-based superconductors, who exhibits the highest $T_c \sim 37$ K in this family.[12] Initially, standard LDA calculations revealed much different and more complex electronic structures due to the hybridization of the 3d orbitals of vanadium. Then, the LDA result brought about the following debate. First, Lee and Pickett argued that the superconductivity of $Sr_2VFeAsO_3$ belongs to a new class different from other families because V d orbitals mix with those of Fe, and break the typical stage as disconnecting Fermi surfaces.[8] On the other hand, Mazin claimed that the relevant spin fluctuation is still alive, similar to those of other iron-based superconductors despite the mixing of V d orbitals.[9] Thus, $Sr_2VFeAsO_3$ can be regarded as a key material to check whether the typical Fermi-surface structure is essential for high-T_c superconductivity. Therefore, we examine whether the electronic structure of $Sr_2VFeAsO_3$ is really different from the typical one in "conventional" iron-based superconductors.

Vanadium oxide is well known to be a strongly correlated system. For instance, V_2O_3 exhibits a phase transition into a Mott insulator at a certain temperature, though standard LDA calculations predict its metallic features.[13] On the other hand, the calculations considering the strong correlation such as LDA+U (Ref. 13) and LDA + dynamical mean-field theory (DMFT) (Ref. 14) succeeded in reproducing the Mott insulating state. The nominal valence of V in V_2O_3 is trivalent, and V in $Sr_2VFeAsO_3$ is naively estimated to be also trivalent from the charge valence. This implies that the perovskite layer including vanadium oxide becomes insulating and then the Fermi surfaces are not influenced by vanadium electrons. In this paper, we explore the electronic structures of $Sr_2VFeAsO_3$ by considering the correlation on 3d vanadium electrons. For this purpose, we use LDA+U method for d electrons of vanadium. As a result, we find that the calculated electronic structure becomes equivalent to those of other iron-based superconductors as expected above, by assuming a checkerboard antiferromagnetic (AFM) order on the vanadium layer. In this case, highly anisotropic electronic structures are also obtained in contrast to the standard calculation results.

The crystal structure of the present target material, $Sr_2VFeAsO_3$ is tetragonal, and the space group of the crystal structure is $P4/nmm$ as shown in Fig. 1. Such a structure is characteristic to the perovskite-type iron-based superconductors but in contrast to most of other family materials whose mother compounds without doping undertake the structural transition into the orthogonal one. This nondoped high-T_c superconductor without the orthogonal transition is relatively convenient for first-principles studies because we do not need to care any doping effect.

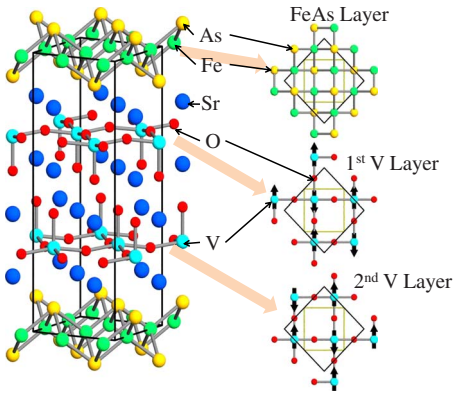

FIG. 1. (Color online) Crystal structure of $Sr_2VFeAsO_3$. The right panel displays each two-dimensional layer seen from c axis. The black small arrows on each V layer denote spin directions in the assumed checkerboard antiferromagnetic order. The small squares in the right panel stand for original unit cell (space group: $P4/nmm$). Thick lines denote the extended unit cell for checker-AFM.

We consider strong correlation on vanadium d-orbital electrons. This is the first trial for the present compound. We point out that it is only a way to reproduce most experimental results consistently. In order to include the strong correlation effect, we use LDA+U method, in which the Hubbard U is applied only on the vanadium d electrons. In our LDA+U calculation, we expect a checker-AFM (c-AF) order on the vanadium layer as a natural consequence of significantly large U. Then, the unit cell is extended to $\sqrt{2}a \times \sqrt{2}a$ in ab plane (see Fig. 1). As a result, the Brillouin zone is folded and the zone corner called M point coincides with the zone center (Γ point). In the calculation unit cell, there are two vanadium layers where checker-AFM orders are arranged as described in Fig. 1. The magnetic order is equivalent to the observed one in $Sr_2CrFeAsO_3$,[15] which does not exhibit superconductivity at all. The difference between these materials is an interesting issue, which will be discussed elsewhere. On the other hand, we do not set any magnetic order for the iron layers except for a case to compare the total energy. The calculation package employed throughout this paper is VASP (Refs. 16 and 17) that supports LDA+U method,[18] in which we choose two parameters, the Hubbard U and Hund's coupling J. While there are methods to calculate the parameters in first-principles manner, e.g., the constrained random-phase approximation,[19] we conventionally treat them as input parameters. Instead, we examine how the electronic structure is affected by various parameter sets. We consider that a combination of $U=5.5$ eV and $J=0.93$ eV is the most reasonable among all sets used in this paper. The set is close to those employed in successful calculations on vanadium oxides using LDA+U and LDA+DMFT.[14,20] The lattice constants and internal coordinate of each atom are in accordance with the experimental data.[12]

Figure 2 shows band dispersions and densities of states calculated by LDA+U method for the four parameter sets, (a) $U=0$, $J=0$, (b) $U=3$ eV, $J=0.93$ eV, (c) $U=5$ eV, $J=0$, and (d) $U=5.5$ eV, $J=0.93$ eV. In all sets of U and J, the checker-AFM order in the vanadium layer is stable, and the calculated moments on vanadium become 1.36 μ_B, 1.65 μ_B, 1.86 μ_B, and 1.79 μ_B for the parameter sets (a)–(d), respectively. In $U=0$, that is, a standard LDA calculation, the bands of spin-down (majority-spin) d electron of vanadium cross the Fermi level as shown in Fig. 2(a), though spin-up bands are away from the Fermi level. In this case, the perovskite layer is not insulating but half metallic as pointed out in Ref. 10. As U increases, the occupied and unoccupied bands of vanadium split and both of those go away from the Fermi level. For reasonable values, i.e., $U=5$ eV and $U=5.5$ eV, they clearly split into upper and lower Hubbard bands, and the blocking layer becomes insulating.

Here, we discuss about the oxidation state of V atoms in the results obtained by LDA+U. In the case of $U=5.5$ eV and $J=0.93$ eV, the occupancy of the d orbitals of V is 2.4, which is almost consistent with the value of V^{3+} ($3d^2$). The small discrepancy from 2 may be caused by the covalency or by ambiguity of the estimated ionic radius of V (the value adopted in this calculation is 1 Å). Figure 3 shows the projected density of states (DOS) of each d orbital of V. The separation between t_{2g} (d_{xy}, d_{yz}, and d_{xz}) and e_g orbitals ($d_{x^2-y^2}$ and $d_{3z^2-r^2}$) are clearly shown in Fig. 3, and the occupied state is dominated by the t_{2g} orbitals. Thus, the first-principles calculations predict trivalent state of V as naively expected above. On the other hand, the possibility of multivalent or pentavalent state is suggested by x-ray photoelectron spectroscopy measurement.[22] However, this experimental result cannot be simply compared to our bulk calculations because of its surface sensitivity.

The Fermi surfaces for the set of $U=5.5$ eV and $J=0.93$ eV are shown in Fig. 4. The surface is formed by only d electrons of iron since the perovskite layer including vanadium is not metallic any longer. In the figure, one finds that all Fermi surfaces are cylindrical around Γ point and two of them are formed as hole pockets and other three as electron ones. We note that the present Brillouin zone is folded because of the checker-AFM ordering of V. As a consequence of the folding, the electron pockets seen in the zone center correspond to those around M point calculated in other iron-based superconducting materials. Thus, we find that the calculated Fermi surfaces are quite equivalent to those of other typical iron-based superconductors. Moreover, our folded result clearly shows that the nesting between those hole and electron pockets is well and the spin fluctuation with the nesting vector is expected to be strongly enhanced. Very recently, Nakayama *et al.* actually reported typical Fermi surfaces as predicted above by using ARPES.[21] This is strong evidence that vanadium $3d$ electrons do not contribute to band structure around the Fermi level, i.e., the vanadium layer is insulating.

In the case of $U=5.5$ eV and $J=0.93$ eV, we also calculate anisotropy of quasiparticle resistivity. Some experimental data qualitatively indicates that the anisotropy is quite large.[22] One of the clearest evidence is the broadening of the superconducting transition by the variation in the applied magnetic field, which is well known on highly anisotropic high-T_c cuprate materials such as $Bi_2Sr_2CaCu_2O_x$ (Bi-2212). The calculated Fermi-velocity anisotropy γ_ρ, defined as $\gamma_\rho = \langle v_a^2 \rangle / \langle v_c^2 \rangle$, becomes 1351 which is much larger than those

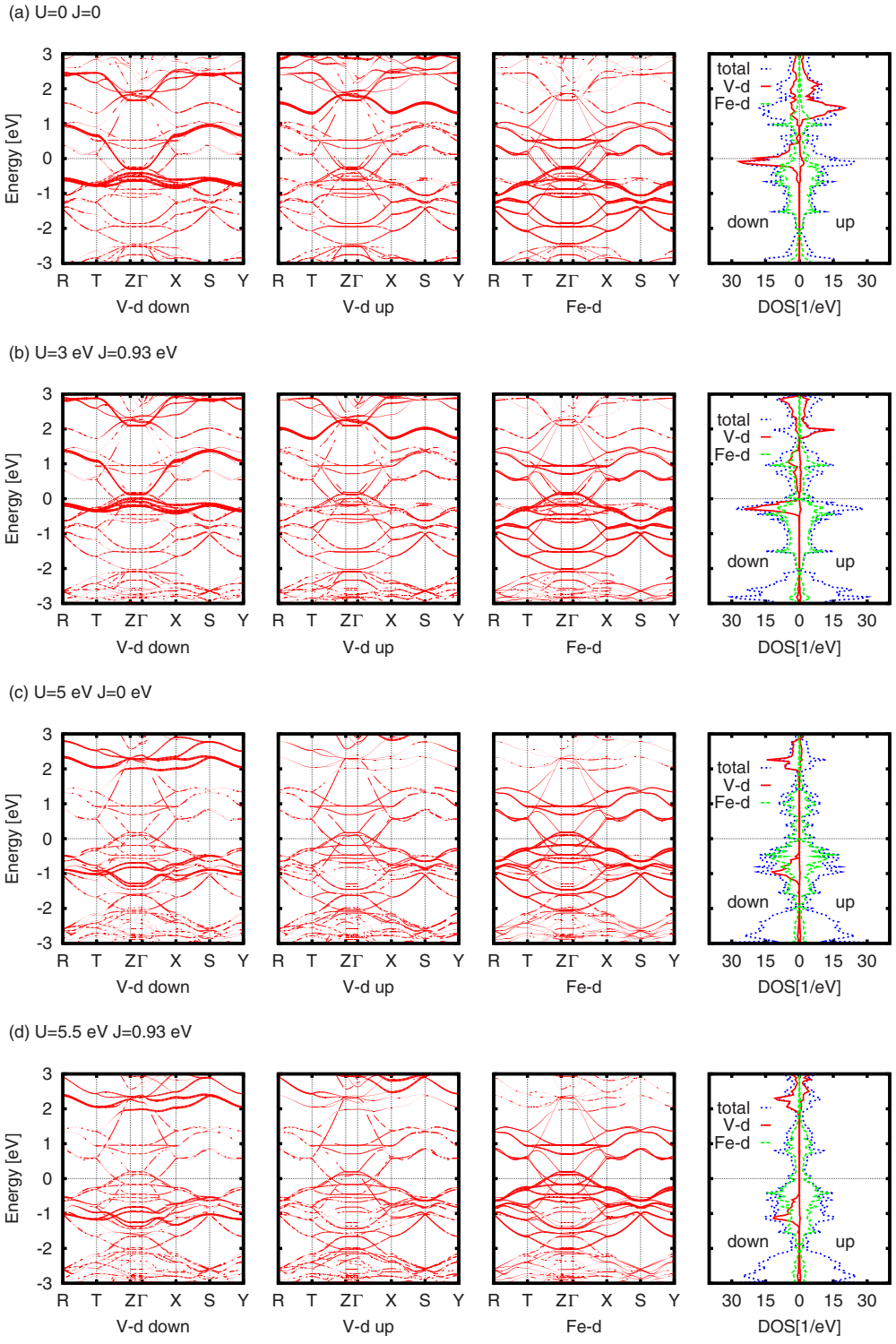

FIG. 2. (Color online) Band structure and density of states calculated by LDA+U for (a) U=0, J=0, (b) U=3 eV, J=0.93 eV, (c) U=5 eV, J=0 eV, and (d) U=5.5 eV, J=0.93 eV. The contributions of V d orbital spin-down, spin-up, and Fe d orbitals to the band dispersions are, respectively, highlighted by bold lines from the left-hand-side panel to the right-hand, in (a)–(d). The total and partial Fe, and partial V DOSs are depicted by the dotted, dashed, and solid curves, respectively, in the right-end panel.

of LaFeAsO (γ_ρ=116.8) and $BaFe_2As_2$ (γ_ρ=10.69) but relatively smaller than perovskite-type $Sr_2ScFePO_3$ (γ_ρ=6.19 $\times 10^5$).[23] The anisotropy of the penetration depth γ_λ at zero temperature is estimated to be ~37 since $\gamma_\lambda=\sqrt{\gamma_\rho}$ at zero temperature. Although the calculated anisotropy is relatively smaller among the family of perovskite-type iron-based superconductors, it is still much larger than other families. Compared to those of high-T_c cuprate superconductors, the anisotropy $\gamma_\lambda \sim 30$ is larger than $YBa_2Cu_3O_{7-x}$ and comparable to $La_{2-x}Sr_xCuO_4$ but smaller than Bi-2212. The value is

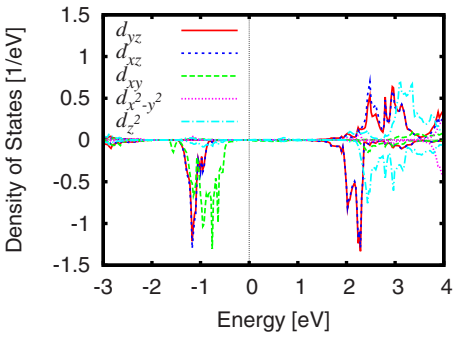

FIG. 3. (Color online) The projected density of states of V d orbitals for the checkerboard antiferromagnetic state calculated by LDA+U with U=5.5 eV and J=0.93 eV. x and y axes are taken to be parallel to V-O-V bondings in a V layer.

fully over the lower bound anisotropy in which intrinsic Josephson effects are observable. In fact, since intrinsic Josephson effects have been confirmed in 1111 systems[24] whose $\gamma_\lambda \sim 10$ according to our first-principles calculations, the expectation is reasonable. Thus, intrinsic Josephson effects are promised. Moreover, we can predict some intrinsic Josephson effects originated from its multiband superconducting gaps. Some literatures report a new excitation called Josephson-Leggett mode in addition to the Josephson plasma due to multitunneling channels,[25] and the others predict new type of Josephson effects originated from the multidegree of freedom of the superconducting phases.[26] At the present, Bi-2212 is intensively investigated to promote the functionality as terahertz wave radiation source. The single crystal of $Sr_2VFeAsO_3$ may work as multiterahertz wave generators due to its multiple excitation modes. See Ref. 23 for those details.

Finally, let us discuss stability of the present checker-AFM state and mention the related issues. We compare the total energy of the c-AF magnetic state with various ordered states from the nonmagnetic (NM) to two magnetic states, ferromagnetic (FM) and antiferromagnetic between V layers (A-AF) (see Fig. 5). The results are summarized in Table I, where all states are calculated by LDA+U with the parameter set, U=5.5 eV and J=0.93 eV. As far as Fe atoms are

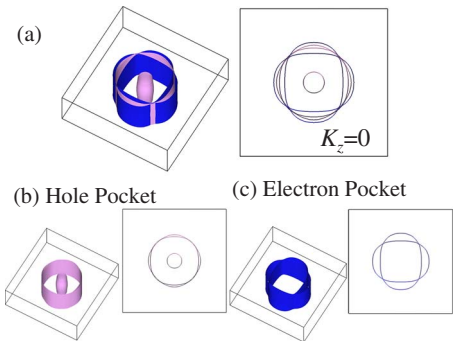

FIG. 4. (Color online) Fermi surfaces for U=5.5 eV and J=0.93 eV. (a) All Fermi surfaces. The dark and light surfaces stand for electron and hole pockets, respectively. The right panel shows a sliced Fermi surface at k_z=0. (b) and (c) describe Fermi surfaces separately for hole and electron pockets, respectively.

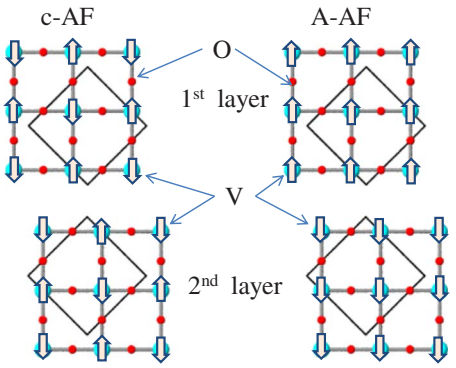

FIG. 5. (Color online) Magnetic order in two V layers of the unit cell (see Fig. 1). Large and small circles denote V and O atoms, respectively. Thick arrows on V atoms show the spin directions and dark squares correspond to the unit cell. Left-side and right-side panels show the checkerboard antiferromagnetic order (c-AF) and antiferromagnetic order between two layers (A-AF), respectively.

nonmagnetic, the energy of the checker-AFM state is the lowest of all calculated ones. This result clearly indicates that the checker-AFM state is the most stable under the application of the Hubbard U on the vanadium d electrons. Very recently, Tatematsu *et al.*, reported that a magnetic transition occurs around 150 K at the vanadium layers by NMR measurement.[27] Although the transition is not yet proved to be the checker-AFM ordering, it can be ascribed to a magnetic ordering at the vanadium layer at least. Otherwise, the transition is attributed to Fe stripe ordering but such ordering drastically changes the Fermi surfaces, which is not consistent with the present ARPES measurement.[21] On the other hand, we have another interesting calculation result, in which the total energy of Fe-stripe AFM together with the checker-AFM of vanadium is lower than that of nonmagnetic Fe with the checker-AFM of vanadium and the most stable of all calculated states as shown in Table I. Then, the calculated Fe

TABLE I. Magnetic moments and total energies for various magnetic orders calculated by LDA+U with U=5.5 eV and J=0.93 eV. NM and FM stand for nonmagnetic and ferromagnetic order, respectively. The antiferromagnetic order between two V layers is denoted by A-AF, the checkerboard antiferromagnetic order in a V layer by c-AF, and the stripe-type antiferromagnetic order in a Fe layer by s-AF. ΔE is the energy difference per formula from that of the most stable state (c-AF and s-AF).

Order		Moments (μ_B)		ΔE
V	Fe	μ_V	μ_{Fe}	(meV)
NM	NM	0	0	2316
FM	NM	1.84	0	186
A-AF	NM	1.85	0	766
c-AF	NM	1.79	0	58
FM	FM	1.90	1.87	847
NM	s-AF	1.87	2.13	430
c-AF	s-AF	1.79	2.12	0

magnetic moment is about 2.1 μ_B, which is comparable to those calculated in most of conventional iron-based superconductors. It is well known that LDA calculations always predict that the stripe-AFM state with Fe moment ~2 μ_B is stable even in the superconducting doping range. This result indicates that the stripe-AFM (Fe) instability on the iron layer strongly works even in $Sr_2VFeAsO_3$ similar to other compounds. Such an agreement is not an accident but a clear evidence for the magnetic instability on Fe layers common to all families of iron-based superconductors.

In conclusions, we calculate the electronic structure of $Sr_2VFeAsO_3$ using LDA+U scheme under an assumption of the checker-AFM ordering on vanadium layers. A reasonable choice of the parameters U and J leads to the insulating blocking layer and typical cylindrical Fermi-surface structures. In addition, our results predict high anisotropy as observed in recent experiments. Consequently, we conclude that the electronic structures are quite equivalent to those of other iron-based superconductors and the similar magnetic instability may contribute to the pairing. Furthermore, the high anisotropy in superconducting transport properties predicts new types of intrinsic Josephson effects originating from the multiband superconductivity. The present result can settle down the controversial problem for the pairing mechanism and suggests a distinct application possibility.

The authors wish to thank K. Terakura and N. Hamada for illuminating discussions in first-principles calculations, and T. Sato, Y. Kobayashi, and Y. Matsuda for stimulating discussions about experimental results. The authors also thank H. Aoki, N. Hayashi, Y. Nagai, M. Okumura, R. Igarashi, Y. Ota, and N. Nakai for valuable discussion. The work was partially supported by Grant-in-Aid for Scientific Research on Priority Area "Physics of new quantum phases in superclean materials" (Grant No. 20029019) from the Ministry of Education, Culture, Sports, Science and Technology of Japan.

*nakamura.hiroki@jaea.go.jp
†machida.masahiko@jaea.go.jp

[1] Y. Kamihara, T. Watanabe, M. Hirano, and H. Hosono, J. Am. Chem. Soc. **130**, 3296 (2008).
[2] M. Rotter, M. Tegel, and D. Johrendt, Phys. Rev. Lett. **101**, 107006 (2008); K. Sasmal, B. Lv, B. Lorenz, A. M. Guloy, F. Chen, Y.-Y. Xue, and C.-W. Chu, *ibid.* **101**, 107007 (2008).
[3] J. H. Tapp, Z. Tang, B. Lv, K. Sasmal, B. Lorenz, P. C. W. Chu, and A. M. Guloy, Phys. Rev. B **78**, 060505 (2008).
[4] F.-C. Hsu, J.-Y. Luo, K.-W. Yeh, T.-K. Chen, T.-W. Huang, P. M. Wu, Y.-C. Lee, Y.-L. Huang, Y.-Y. Chu, D.-C. Yan, and M.-K. Wu, Proc. Natl. Acad. Sci. U.S.A. **105**, 14262 (2008).
[5] See, e.g., K. Ishida, Y. Nakai, and H. Hosono, J. Phys. Soc. Jpn. **78**, 062001 (2009), and references therein.
[6] K. Kuroki, H. Usui, S. Onari, R. Arita, and H. Aoki, Phys. Rev. B **79**, 224511 (2009), see also references therein.
[7] H. Ogino, Y. Matsumura, Y. Katsura, K. Ushiyama, S. Horii, K. Kishio, and J. Shimoyama, Supercond. Sci. Technol. **22**, 075008 (2009).
[8] K.-W. Lee and W. E. Pickett, EPL **89**, 57008 (2010).
[9] I. I. Mazin, Phys. Rev. B **81**, 020507(R) (2010).
[10] I. R. Shein and A. L. Ivanovskii, J. Supercond. Novel Magn. **22**, 613 (2009).
[11] G. Wang, M. Zhang, L. Zheng, and Z. Yang, Phys. Rev. B **80**, 184501 (2009).
[12] X. Zhu, F. Han, G. Mu, P. Cheng, B. Shen, B. Zeng, and H.-H. Wen, Phys. Rev. B **79**, 220512(R) (2009).
[13] S. Yu. Ezhov, V. I. Anisimov, D. I. Khomskii, and G. A. Sawatzky, Phys. Rev. Lett. **83**, 4136 (1999).
[14] K. Held, G. Keller, V. Eyert, D. Vollhardt, and V. I. Anisimov, Phys. Rev. Lett. **86**, 5345 (2001).
[15] M. Tegel, F. Hummel, Y. Su, T. Chatterji, M. Brunelli, and D. Johrendt, EPL **89**, 37006 (2010).
[16] G. Kresse and J. Hafner, Phys. Rev. B **47**, 558 (1993); G. Kresse and J. Furthmüller, Comput. Mater. Sci. **6**, 15 (1996); Phys. Rev. B **54**, 11169 (1996).
[17] In our calculations, we use the projector augmented wave method (Ref. 28) with generalized gradient approximation exchange-correlation energy (Ref. 29). K points are taken as $8\times8\times3$ for self-consistent loop and $10\times10\times4$ for density of states. Self-consistent loop is repeated until the energy difference between loops becomes less than 10^{-7} eV.
[18] A. I. Liechtenstein, V. I. Anisimov, and J. Zaanen, Phys. Rev. B **52**, R5467 (1995).
[19] K. Nakamura, R. Arita, and M. Imada, J. Phys. Soc. Jpn. **77**, 093711 (2008).
[20] I. Solovyev, N. Hamada, and K. Terakura, Phys. Rev. B **53**, 7158 (1996).
[21] T. Qian, N. Xu, Y. B. Shi, K. Nakayama, P. Richard, T. Kawahara, T. Sato, T. Takahashi, M. Neupane, Y. M. Xu, G. Xu, X. Dai, Z. Fang, P. Cheng, H. H. Wen, and H. Ding (unpublished).
[22] F. Han, X. Zhu, G. Mu, P. Cheng, B. Shen, B. Zeng, and H. Wen, Sci. China, Ser. G **53**, 1202 (2010).
[23] H. Nakamura, M. Machida, T. Koyama, and N. Hamada, J. Phys. Soc. Jpn. **78**, 123712 (2009).
[24] H. Kashiwaya, K. Shirai, T. Matsumoto, H. Shibata, H. Kambara, M. Ishikado, H. Eisaki, Y. Iyo, S. Shamoto, I. Kurosawa, and S. Kashiwaya, Appl. Phys. Lett. **96**, 202504 (2010).
[25] Y. Ota, M. Machida, T. Koyama, and H. Matsumoto, Phys. Rev. Lett. **102**, 237003 (2009).
[26] I. B. Sperstad, J. Linder, and A. Sudbø, Phys. Rev. B **80**, 144507 (2009); D. Inotani and Y. Ohashi, *ibid.* **79**, 224527 (2009); Y. Ota, M. Machida, T. Koyama, and H. Matsumoto, *ibid.* **81**, 014502 (2010).
[27] S. Tatematsu, S. Asai, E. Satomi, Y. Kobayashi, and M. Sato, Meeting of Physical Society of Japan, 2010 (unpublished).
[28] P. E. Blöchl, Phys. Rev. B **50**, 17953 (1994); G. Kresse and D. Joubert, *ibid.* **59**, 1758 (1999).
[29] J. P. Perdew, K. Burke, and M. Ernzerhof, Phys. Rev. Lett. **77**, 3865 (1996).